Colloid and Interface Science Communications 42 (2021) 100395

Contents lists available at ScienceDirect

Colloid and Interface Science Communications

journal homepage: www.elsevier.com/locate/colcom

Tailoring the dispersibility of non-covalent functionalized multi-walled carbon nanotube (MWCNT) nanosuspension using shellac (SL) bio-resin: Structure-property relationship and cytotoxicity of shellac coated carbon nanotubes (SLCNTs)

A.K.M. Moshiul Alam [a,b,*], M.D.H. Beg [b,*], R.M. Yunus [b], M.R. Islam [a], Quazi T.H. Shubhra [c,**]

[a] Institute of radiation and Polymer Technology, Bangladesh Atomic Energy Commission, Dhaka 1000, Bangladesh
[b] Faculty of Chemical and Natural Resources Engineering, Universiti Malaysia Pahang, Kuantan 26300, Malaysia
[c] Key Laboratory of Oral Medicine, Guangzhou Institute of Oral Disease, Stomatology Hospital of Guangzhou Medical University, Guangzhou 510140, China

ARTICLE INFO

Keywords:
Multi-walled carbon nanotube (MWCNT)
Shellac (SL)
Nanocomposites
Microstructure analysis
Cytotoxicity
ROS (reactive oxygen species)

ABSTRACT

This study first reports the use of natural thermoplastic bio-resin shellac (SL) to functionalize multi-walled carbon nanotubes (MWCNTs). The MWCNTs were coated with 5, 10, and 15 wt% SL solutions to fabricate SLCNT nanocomposites which are highly dispersible and stable in solution. Enhanced surface charge imparted long-term stabilization of SLCNT nanosuspension. Microscopic analysis revealed distinct dispersion of nanotubes and a thin layer of SL on the surface of nanotubes in the nanocomposite system. FTIR and Raman spectroscopy confirmed well interaction between SL and MWCNT in the nanocomposites. It was disclosed by the microstructure analysis that the SL concentration affects the lattice parameters of SLCNT nanocomposites. The thermal stability of SLCNT was impressive compared to MWCNT. According to the ROS (reactive oxygen species) generation profile and cell viability study, SLCNTs have reduced adverse effects on cells. Therefore, the results confirm that shellac can significantly improve the stability of MWCNT and reduce the cytotoxicity to facilitate their widespread applications.

1. Introduction

To date, carbon nanotubes (CNTs) have attracted numerous researchers in the arena of nanotechnology including transistors, sensors, energy storage, electrochemical supercapacitors, nanoprobes, composite materials, nanomedicine, etc. due to their distinctive properties. They exhibit considerable architecture, hydrophobicity, photosensitivity and conductivity. CNTs show very good mechanical properties and they also demonstrate antibacterial activity [1]. Their size make them very suitable for many applications [2,3]. CNTs possess all the required chemical, electrical, mechanical, and thermal properties to become ideal electronic materials for next-generation electronic devices [4,5]. In the structure of CNT, the hollowness and extended surface area to volume ratio are suitable for drug loading and delivery which make them attractive candidate for the treatment of various diseases [6]. CNTs especially 'smart' CNTs have already shown promising results in cancer treatment [7]. The biological macromolecules, such as DNA, RNA, and protein remain intact in the hydrophobic CNT reinforced bio-membrane and can be delivered to target cells without harming the adjacent cells [8,9]. CNTs are also very effective adsorbent and have been investigated for the adsorptive removal of environmental pollutants including various heavy metal ions from aqueous solutions [10,11].

However, the major limitations of CNTs are low dispersibility and poor functionality which restrict their biomedical applications. These limitations can be overcome using polymers by covalent and non-covalent functionalizations. Previously, we have reported several works on surface modifications to improve the functionality of materials [12,13]. The covalent functionalization method is popular concerning the non-covalent functionalization of CNT. However, it produces defects due to chemical bonding to the structure of CNT; therefore, changes the optical, thermal, and other useful properties of CNT [14]. Nevertheless, functionalization of CNT is the most effective strategy to significantly

* Corresponding authors at: Faculty of Chemical and Natural Resources Engineering, Universiti Malaysia Pahang, Kuantan 26300, Malaysia.
** Corresponding author.
E-mail addresses: akmmalam@gmail.com (A.K.M.M. Alam), dhbeg@yahoo.com (M.D.H. Beg), shubhro.du@gmail.com (Q.T.H. Shubhra).

https://doi.org/10.1016/j.colcom.2021.100395
Received 7 December 2020; Received in revised form 7 March 2021; Accepted 8 March 2021
Available online 21 March 2021

reduce their cytotoxicity facilitating their in vivo applications.

The non-covalent method is nondestructive and accomplished by the interaction between CNTs and macro- or supramolecules through polymer wrapping or adsorption [15,16]. The possibility of damage in the structure of CNT is completely reduced by non-covalent method. However, the main disadvantage of non-covalent method is the low functionality of CNT. The consequence is the limited application of CNT in biomedical area [14].

Shellac is a special natural bio-resin secreted from lac insects which contains different laccaic acids. Usually, it is composed of a single ester-containing hydroxyl and carboxylic groups [17]. The film-forming and barrier characteristics shown by shellac is remarkable. In the last few decades, it has got a remarkable application in the food and agro-industries to enhance the shelf life [18,19]. In the pharmaceutical industries, shellac is familiar with the drug delivery systems due to its biocompatible and biodegradable properties as well as fewer side effects [20,21]. Currently, in absence of any other reagent, shellac is used as a non-toxic reducing and stabilizing agent of gold nanoparticles [17]. Shellac is biocompatible as well as an edible natural material which can be used to fabricate sustainable organic field-effect transistor for developments of bio-integration applications [22]. In drug formulation, the biocompatible and biodegradable shellac enteric coating is used in the oral drug delivery process. Shellac nanofiber has been used for stimuli-responsive release of ferulic acid as an antioxidant [23–25]. Besides, shellac coating protect tablets from moisture, humidity, or air oxidation [26]. In bone tissue engineering, the biocompatible shellac has been employed to fabricate hydroxyapatite-shellac-sugar bio-composites which was used as bone filler materials [27].

To best of our knowledge, there is no report on MWCNT functionalization using shellac bio-resin. Hence, we utilized multifunctional shellac macromolecules and adsorbed them on the surface of CNTs to improve the dispersibility and functionality of nanotubes. It is noteworthy to emphasize that SL coating is not only great in improving the stability of CNT in dispersion, it also greatly influences dispersed CNT's properties that can facilitate their application. e.g., in the biomedical field by reducing cytotoxicity. SL coating can improve the thermal stability of CNT which was evident from our TGA (thermogravimetric analysis) study. Moreover, SL coating can remove most of the impurities from CNT and can reduce cytotoxicity as was evident from the cell viability study of this research. Based on many studies it is obvious that CNT is an excellent carrier as a nano-drug delivery system. To utilize as a carrier, CNT needs to be modified to interact with drug molecules as well as to stay stable in the solution. But during modification, the CNT surface gets defected due to chemical bonding and electronic configuration also changes. As a result, CNT becomes toxic. On the other hand, CNT modification without defect by surface coating or wrapping using the non-covalent technique is familiar, but the functionality and stabilization are poor to deliver the drug molecules. Therefore, the objectives of this work are the achievement of high stabilization of CNT using shellac solution and to evaluate dispersibility of shellac coated CNT nanocomposites along with the possible effect of SL on the CNT structure.

2. Materials and methods

2.1. Materials

Multi-walled carbon nanotubes (MWCNTs), produced by moving-bed catalysis technique having diameter < 8 nm, length between 10 and 30 μm, and carbon purity of 95%, was purchased from Timesnano, China. Polish grade shellac was purchased from the farmer market of Chapainowabgonj district, Bangladesh. Tetrahydrofuran (THF), methanol, ethanol, and acetone solvents were purchased from Merk, Germany. DMEM, MTT assay kit, and 2′,7′-dichlorofluorescin diacetate (DCFH-DA) was purchased from Life Technologies, Thermo Fisher, and Sigma-Aldrich, respectively. All chemicals and solvents were of analytical grade.

2.2. Methods

2.2.1. Dispersion of CNT in shellac solution and fabrication of shellac coated CNT nanocomposites (SLCNT)

We first performed some preliminary studies and observed that shellac concentration is crucial to stabilize MWCNTs. Our primary attempts utilizing 0.25, 0.5, 0.75, and 1% (by wt) shellac solution to stabilize MWCNT failed to result in well dispersion of MWCNTs (data not shown here). In this research, 5% shellac (wt% with respect to the weight of MWCNT) was dissolved in THF solvent to produce shellac solution. In the same way, we also prepared 10 and 15% shellac solutions. At first, the shellac solution was diluted to a concentration of 2 mg/ml. Oven-dried MWCNT was pre-dispersed in THF solvent maintaining a ratio of CNT to THF (wt/vol) 1: 10. The suspension was sonicated for 1.5 h in an ice cube filled ultrasound bath. The pre-dispersed MWCNT suspension was then added to the shellac solution. The suspension of MWCNT and shellac solution was stirred by a magnetic stirrer at 1500 rpm for 15 min followed by 1.5 h of sonication to achieve homogeneous dispersion of MWCNT. The dispersions of shellac-MWCNT were stored in different transparent reagent bottles to observe the sedimentation of MWCNT at different time intervals. Finally, THF solvent was evaporated at 66 °C to get SLCNT1, SLCNT2, SLCNT3 nanocomposites containing 5, 10, and 15 wt% shellac, respectively. All three nanocomposites were dried in a vacuum oven at 100 °C for 18 h. The SLCNT nanocomposites were subjected to various analyses to evaluate the structure and properties of the nanocomposites. We also investigated the adverse effects of SLCNTs and MWCNTs on macrophage cells.

2.3. Characterization

2.3.1. Viscosity

The viscosity of CNT nanosuspension in shellac solution was measured by the Brookfield DV-III ULTRA, digital rotary viscometer according to ASTM D2983. The average viscosity of five measurements was recorded in the unit of mPa·s.

2.3.2. Zeta potential measurement

The absolute zeta potential (ZP; denoted by ζ) was measured using Zetasizer Nano ZS (Malvern Instruments, Malvern, UK) at 25 °C. For each sample, three parallel measurements were carried out and the mean of the three measurements was calculated. Samples were centrifuged, supernatants were discarded and re-dispersed in the same volume of distilled water by sonication.

2.3.3. Electron microscopic analyses

The surface morphologies of pristine MWCNT and SLCNT nanocomposites were investigated by a transmission electron microscope (TEM) (JEOL Co. JEM1400, accelerating voltage 100 kV).

Moreover, the surface morphology of pristine MWCNT, SLCNT nanocomposites were studied by the field emission scanning electron microscope (FESEM) (JOEL, JSM-7800 F, Japan). Samples were mounted on aluminium stubs with carbon tape followed by a sputter coating with platinum to make them conductive before analyzing them by FESEM.

2.3.4. Fourier-transform infrared (FTIR) analysis

Solid shellac, MWCNT, and SLCNT powders were subjected to the Fourier-transform infrared (FTIR) spectroscopy analysis. The analyses were carried out on a Nicolet 6700 FT-IR spectrometer (Thermo Scientific, Germany) using the standard attenuated total reflection (ATR) technique. The spectra were collected from 4000 to 500 cm^{-1} with a 4 cm^{-1} resolution over 50 scans.

2.3.5. Raman analysis

MWCNT and SLCNT powders were subjected to the Raman spectroscopy analysis using Jasco Co. NR-1800. The laser $\lambda = 532$ nm was

used for excitation to obtain the Raman spectra.

2.3.6. X-ray diffraction (XRD) analysis

X-ray diffraction (XRD) analysis was performed by Rigaku Mini Flex II, Japan (operated at 30 kV and 15 mA). The specimens were stepwise scanned over the operational range of scattering angle (2θ) from 3 to 40°, with a step of 0.02°, using CuK_α radiation of wavelength $\lambda = 1.541$ Å. The data were recorded in terms of the diffracted X-ray intensities (I) versus scattering angle (2θ). The crystallographic spacing (d) was calculated by following Bragg's Eq. (1).

$$\lambda = 2dsin\theta \quad (1)$$

The average size of the crystallites, z, was determined with the full width at half-maximum (FWHM) of XRD peak by using the following Scherer's Eq. (2):

$$z = \frac{0.9\lambda}{\delta Cos\theta} \quad (2)$$

Where δ is the FWHM (in radians) and θ is the diffraction angle. The δ value was determined by curve fitting after subtracting the amorphous background. The Gaussian curve was fitted at the top of the peak for determining δ and the position using an appropriate program. The lattice strain (χ) was evaluated using the Williamson–Hall Eq. (3).

$$\chi = \frac{\delta}{4tan\theta} \quad (3)$$

2.3.7. Thermal analysis

Thermogravimetric analysis (TGA) was performed by TGA (Q500 V6.4, Germany) in a platinum crucible under nitrogen atmosphere with a heating rate of 10 °C/min. The temperature range was scanned from 20 to 700 °C.

2.3.8. In vitro analyses

2.3.8.1. Cell culture. RAW 264.7 macrophage cells were used in this study to investigate the effect of SL modification on the cell viability over untreated MWCNT. Cells were cultured in DMEM (Life Technologies) supplemented with 10% FBS (fetal bovine serum, Life Technologies) and 100 μg/ml penicillin and 100 μg/ml streptomycin at 37 °C in a humidified atmosphere (5% CO_2).

2.3.8.2. Measurement of intracellular reactive oxygen species (ROS). The intracellular ROS determination was carried out using 2′,7′-dichlorofluorescin diacetate (DCFH-DA). DCFH-DA reacts with ROS inside the cells and oxidized to form highly fluorescent compound dichlorofluorescein (DCF). Briefly, 1×10^4 cells were seeded in a 96 well plate and cultured for 24 h. Thereafter, we added MWCNTs and SLCNTs (5, 25, 100, 250, 500 μg/ml) and incubated the cells for another 24 h. After the treatment period, we washed the cells three times with PBS, added DCHF-DA (10 μM), and incubated for 30 min in dark at 37 °C. Finally, cells were washed again three times with PBS and the fluorescence intensity was measure using a spectrofluorometer (Ex: 488/Em: 520 nm).

2.3.8.3. Cytotoxicity study. Cell viability was examined using MTT [3-(4,5-dimethylthiazol-2-yl)-2,5-diphenyltetrazolium bromide] assay. We followed the protocol provided by the manufacturer and followed our previous study too [28,29]. Briefly, cells (1×10^4 cells) were seeded and precultured for 24 h. Thereafter, MWCNT and SLCNT of different concentrations (5, 25, 100, 250, 500 μg/ml) were added to the cells and incubated for another 24 h before investigating their viability by MTT assay. Positive control cells were cultured for 48 h without any nanotubes. Cell viability is expressed as the percentage (%) of absorbance relative to the positive control (cells cultured with no nanotubes) and absorbance of MTT treated cells was determined at 570 nm using a microplate reader.

2.3.9. Statistical analyses

Data from three independent sample solutions were expressed as means ± standard deviations (SD). Differences were identified using a Student's t-test and were considered significant when $p < 0.05$.

3. Results and discussion

3.1. Stability of the prepared dispersion and suspension

3.1.1. Photophysical observation

As stated earlier, shellac concentration is crucial to stabilize MWCNTs, and concentration up to even 1% (by wt) shellac solution cannot stabilize MWCNT showing poor dispersion and quick aggregation. Photographs shown in Fig. 1(a)–(c) illustrate three different solutions: (a) neat 5% shellac solution in THF solvent, (b) MWCNT suspension in THF solvent, and (c) MWCNT dispersion in 5% shellac solution. The suspension shown in Fig. 1(b) loses its dark color after 3–4 h of post sonication due to the aggregation of MWCNT resulting in distinguishable sediment which can be observed by naked eyes. In contrary, the dark color of MWCNT dispersion in shellac solution (Fig. 1 (c)) was quite stable and was almost unchanged in color with no visible sediment.

Three parallel nanosuspensions of MWCNT in shellac solution were prepared, stored at room temperature for 14 days and the sedimentation behavior of the MWCNT nanosuspensions was monitored periodically for up to 14 days. Surprisingly, there was no visible aggregation of MWCNT in shellac solution even at the end of 14 days of storage time. This observation indicates that the MWCNTs acquire prolonged stability in our shellac solution. Furthermore, the physicochemical properties of MWCNT nanosuspension in shellac solution were investigated (by the rheology, and particle size distribution) which strongly supported our visual observation.

3.1.2. Surface charge analysis

It is well known that MWCNTs have a strong tendency to form bundles due to their high aspect ratio and high flexibility plus strong van der Waals forces. Pristine MWCNTs used in this study had no charge. Hence, they were hydrophobic, poorly dispersed in water, and got aggregated. Polymers or surfactants are commonly used to non-covalently functionalize MWCNTs by physisorption of molecules which prevent bundling or twisting of MWCNTs avoiding a change of graphitic structure. Shellac is a biopolymer having both carboxyl and hydroxyl groups as can be seen from their chemical structure shown in Fig. 1(d). Hence, adsorption of shellac molecules on MWCNTs introduce carboxyl and hydroxyl groups on the surface of MWCNTs. The presence of these two groups on the MWCNT surface changes their wettability which results in better dispersion of MWCNTs in solution due to electrostatic repulsion exhibited in Fig. 1(e).

To understand the stability of unmodified and shellac modified MWCNTs, the zeta potential was measured to investigate the surface charge of their colloidal solutions. ZP values of unmodified and 5, 10, and 15% shellac modified MWCNTs were 23 ± 1.5, 35 ± 4.2, 45 ± 1.9, and 53 ± 3.4 mV, respectively. To understand the stability based on ZP values, Table S1 can be helpful [30]. Moreover, the ASTM standard (ASTM1985) suggests that the absolute value of ZP if lower than ±25 mV, van der Waals attraction among the particles cannot be overcome by the repulsive force and particles must aggregate [31]. Based on the values, we can easily understand that unmodified MWCNTs were unstable which supports our visual observation as was shown in Fig. 1(b). In contrary, ZP values of SLCNTs indicate that they were quite stable which were also observed visually (Fig. 1(c)). An increase in shellac concentration provides an increased number of shellac molecules in the solution and thereby increases the driving force for shellac adsorption on the MWCNT surfaces.

If the solution pH is shifted to the alkaline range by adding NaOH to the solution, sedimentation is observed for SLCNTs which supports the

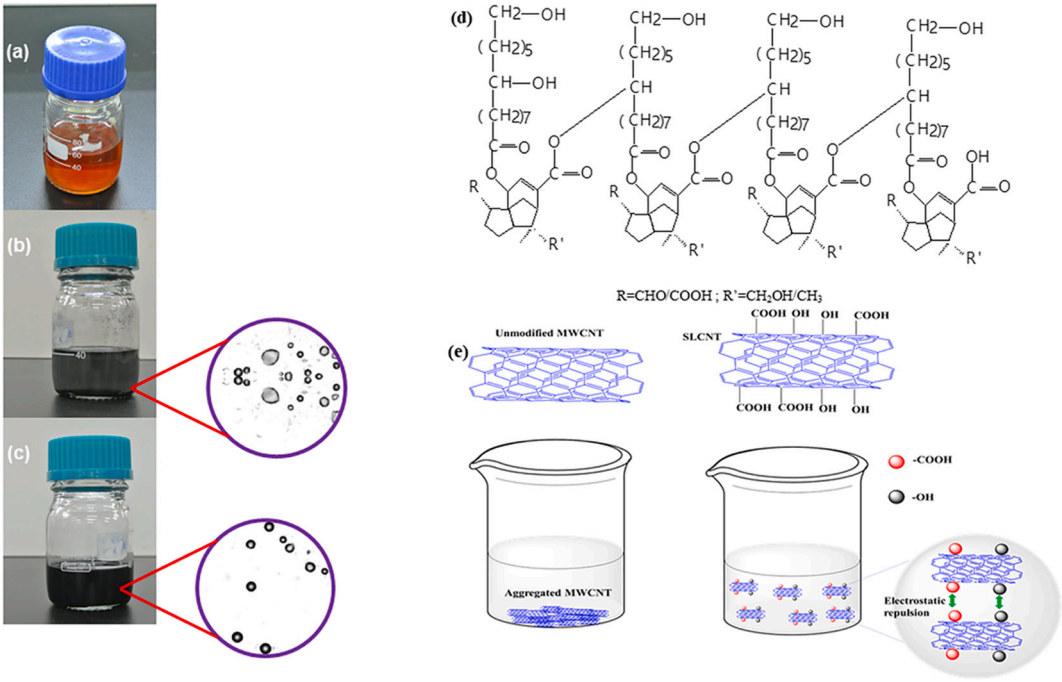

Fig. 1. Photophysical observation of (a) shellac solution, (b) MWCNT in THF, and (c) MWCNT in shellac solution, (d) schematic chemical structure of a shellac bio-resin molecule, and (e) schematic representation of aggregation of unmodified MWCNT (left), dispersion of SLCNT (middle), and electrostatic repulsion due to the presence of -COOH and -OH groups on SLCNT (right).

presence of hydroxyl and carboxyl groups on their surface.

3.1.3. *Viscosity analysis*

The rate of sedimentation of nanoparticles is dependent on the viscosity of the medium, size, and density. Dispersions with inter-particle repulsion can exhibit higher viscosity compared to the sedimented solutions since the density of liquid decreases due to settlement of particles by sedimentation. Hence, investigation of the viscosity of nanosuspensions was carried out to better understand their stability behavior. Fig. 2 reveals the viscosity of MWCNT nanosuspensions as a function of (a) shellac concentration, and (b) storage time. In the case of different shellac concentration with fixed weight of MWCNT, the measurement was performed after 15 min of sonication. The viscosity of the nanosuspensions showed a sharp increase with the increase in shellac concentration. It is obvious that despite a fixed quantity of MWCNT and a constant shear rate, the population of shellac molecules increases with the increase in shellac quantity which affected the viscosities of the nanosuspensions. Additionally, the percolated structure of MWCNT remains unchanged at that shear rate due to increased viscosity of nanosuspension at a higher concentration of shellac [32].

It is well known that with the increase in polymer concentration in the solution, viscosity increases. Moreover, at high concentration, more shellac molecules interact with MWCNT which is another reason behind increased viscosity [33]. Therefore, the lowest concentration (5 wt% in this study) of shellac is considered as an adequate quantity to form low viscous and well dispersed MWCNT nanosuspension.

Fig. 2(b) represents the viscosities of MWCNT dispersion having 5 wt % shellac relative to the MWCNT content for different storage periods. The viscosity was measured at a constant shear rate which slightly decreased with increasing storage time. Usually, an increase in the particle size and sediment volume lead reduction in the viscosity of nanosuspension as stated elsewhere [34]. There was no drastic change or a sharp drop in viscosity over the storage period indicating no or slight sedimentation. The trend of viscosity change certainly supports well dispersion as well as longtime stabilization of MWCNT in the shellac solution which ultimately complies with Fig. 1(c). Hence, we can conclude from the above observations that prolong stabilization of MWCNT was achieved in the shellac solution.

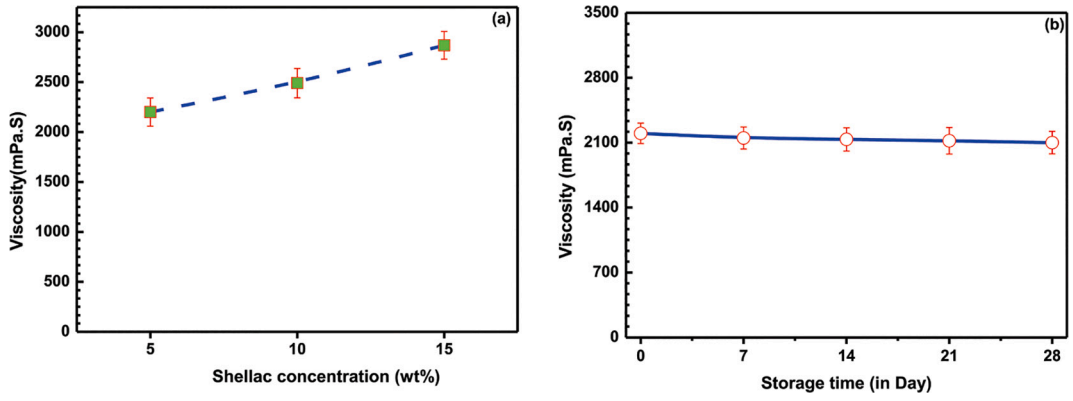

Fig. 2. Viscosity of dispersed MWCNT as a function of (a) shellac concentration and (b) storage time.

3.2. Electron microscopic analyses

For in-depth investigation of the morphology of our nanocomposite samples, we performed electron microscopic analyses. FESEM images shown in Fig. 3(a) demonstrate the dispersion of (i) pristine MWCNT and (ii) SLCNT nanocomposites.

It is obvious that pristine MWCNTs exist in a compact large lump, individual nanotube is thick like rope due to the twisting of several nanotubes. In contrary, it was found that the SLCNTs exist individually in a well-dispersed manner. It is quite possible to distinguish most of the nanotubes like thin yearn. Furthermore, it is noticeable that most of the nanotubes are disentangled from each other. The thinnest nanotubes like spider knit yearn are interconnected with each other in the micrograph.

Fig. 3(b) illustrates the TEM micrographs of (i) MWCNT and (ii) SLCNT nanocomposites. The disentangled as well as well distributed nanotubes are visible in the image (b) of SLCNT nanocomposites. On the other hand, entangled and agglomerated MWCNTs are noticeable in Fig. 3(b)(i). Additionally, the thick surface is clearly visible on SLCNT nanotubes compared to the surface of pristine MWCNTs. This observation indicates the interaction of shellac molecules with the surface of nanotubes in the SLCNT nanocomposite system. Therefore, cohesive force or the van der Waals force reduced which disentangled nanotubes in the SLCNT nanocomposites and perhaps resulted in long-time stabilization of nanotubes in dispersion [35].

3.3. FTIR analysis

The attachment of SL on the MWCNT surface imparts negative charge and introduces carboxyl and hydroxyl groups on their surface as was shown in Fig. 1(e) and indicated by zeta potential value. To investigate the chemical interaction between the nanoparticles and grafted molecules, FTIR is a very effective tool. FTIR spectra of pristine MWCNT, SL, and SLCNT nanocomposites are shown in Fig. 4(a). The spectrum of pure shellac exhibits the presence of carboxyl (-COOH) functional groups, alkane linkage in the shellac molecule.

The peaks appeared at 1705 cm^{-1}, 1605 cm^{-1}, 2852 cm^{-1} corresponding to the >C=O, cyclic C—C, and C—H stretching of alkane in the shellac molecule. The sharp peak appearing at 1245–1019 cm^{-1} corresponds to C—O stretching which confirms the presence of ester linkage in the shellac molecules [33]. The peak that appeared at 2920 cm^{-1} is due to the O—H stretching of the -COOH group in the shellac molecule. The broad peak at 3332 cm^{-1} reveals the hydrogen-bonded O—H stretching in the shellac molecule. Shellac is an ester molecule that contains hydroxyl group, hydrocarbon chain and carbon ring (chemical structure (Fig. 1(d)) and FTIR spectrum confirmed them.

The spectrum of pristine MWCNT exhibits the C—C stretching of nanotubes in the range of 1620–1600 cm^{-1}. Additionally, the presence of hydroxyl moieties on the surface of nanotubes and the corresponding peaks appeared in the range of 3500–3190 cm^{-1}. Moreover, the peaks that appeared at around 1300–950 cm^{-1} are due to oxygen and hydrogen-based functional groups that were present as impurities in the supplied MWCNT.

In case of SLCNT, the peak sharpness at 3443 cm^{-1} reveals that alcoholic -OH groups are hydrogen-bonded and anchored onto the surface of MWCNT.

The perceptible uniform peak of >C=O group is shifted towards the lower wavenumber at 1636 cm^{-1} because of the strong interaction of shellac molecule with MWCNT. It suggests that loan pair electrons, as well as π electrons of the carbonyl group, undergo electrostatic interaction with MWCNT [36]. Furthermore, the ester-linked C—O peak shifts towards the shorter wavelength from 1245 cm^{-1} to 1115 cm^{-1} and this blue shift confirms the strong interaction between shellac and MWCNT. A summary of the observed peaks in terms of wavenumber corresponding to the mode of vibration of bonds is presented in Table S2.

3.4. Raman analysis

The comparative Raman spectra of pristine MWCNT and shellac coated SLCNT nanocomposites are illustrated in Fig. 4(b). They exhibit graphite mode G band and disorder-induced mode D band. The

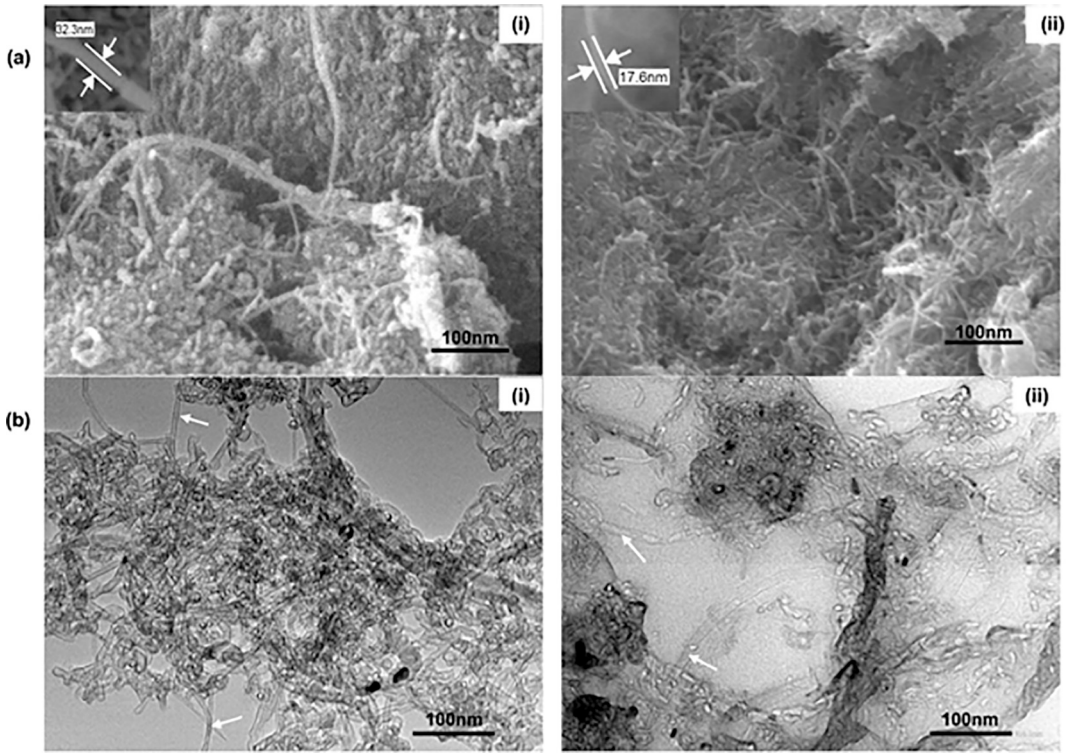

Fig. 3. (a) FESEM micrographs of (i) MWCNT and (ii) SLCNT nanocomposites, (b) TEM micrographs of (i) MWCNT and (ii) SLCNT nanocomposites.

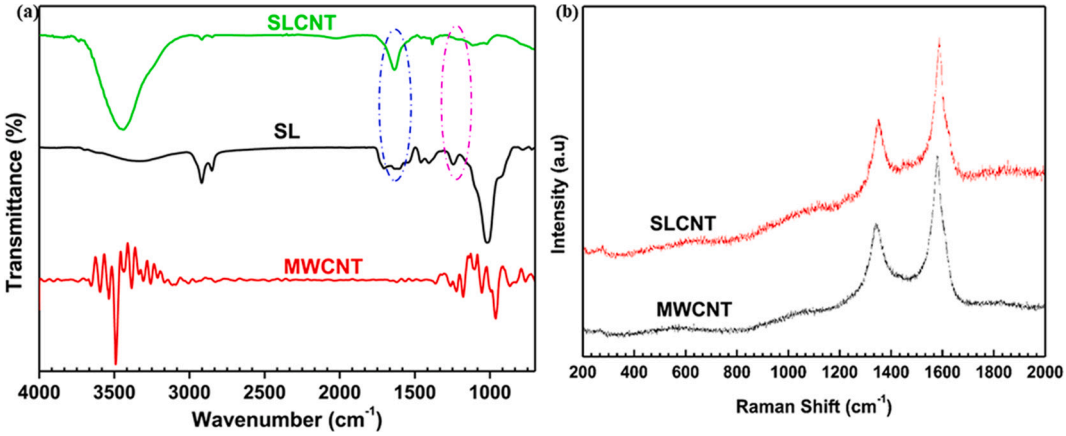

Fig. 4. (a) FTIR spectra of MWCNT, SL and SLCNT, (b) Raman spectra of MWCNT and SLCNT.

corresponding G band indicates the C—C stretching vibration in MWCNT and SLCNT at around 1580 and 1587 cm^{-1}. The D band of MWCNT and SLCNT appears at around 1345 cm^{-1} and 1351 cm^{-1}, respectively. The G band's shifting towards +7 cm^{-1} for SLCNT indicate the attachment of shellac molecules on the surface of the MWCNT [37,38]. Additionally, the corresponding D band and G band intensity ratios of MWCNT and SLCNT were 0.81 and 0.85 which reveal that the shellac molecules covered the MWCNT surface in SLCNT nanocomposites.

3.5. Microstructure analysis

The X-ray diffractograms of neat Shellac (SL), pristine MWCNT, and SLCNT nanocomposites are presented in Fig. 5. Table 1 illustrates the values of scattering angles (2θ), full width at half maximum(δ), lattice spacing (*d*), crystallite size (z), and lattice strain (χ) of those specimens. The diffraction pattern of SL notices the narrowest intense peak at 2θ = 21.687° corresponding to the (110) phase. The diffraction of SL attributes the largest crystal, highest lattice space, lowest lattice strain, and might exist the lowest stacking fault among the specimens. The Pristine MWCNT exhibits a broad diffraction peak that appears at 2θ = 25.71° corresponding to the (002) phase. The widening of pristine nanotubes peak is due to small crystallite size, some staking fault and non-uniform lattice strain in nanotubes. Additionally, pristine nanotubes might be an inhomogeneous mixture of amorphous carbon materials and other impurities and as a consequence X-ray diffraction peak became wide [39,40].

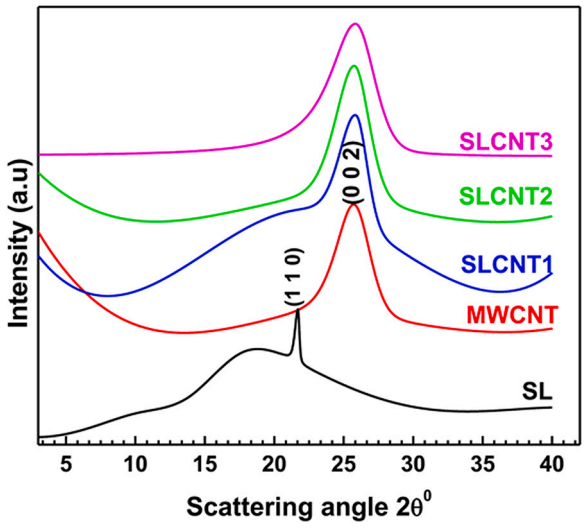

Fig. 5. X-ray diffractograms of neat shellac, pristine MWCNT, SLCNT1, SLCNT2, SLCNT3 nanocomposites.

Table 1
Diffraction and lattice parameters of SL, MWCNT and SLCNT nanocomposites.

Sample name	2θ (°)	θ (°)	δ (°)	λ Å	*d* Å	z(nm)	χ
SL	21.687	10.843	0.361	1.541	4.095	22.511	0.471
MWCNT	25.71	12.855	2.92		3.463	2.792	3.20
SLCNT1	25.86	12.93	2.33		3.443	3.499	2.54
SLCNT2	25.74	12.87	2.95		3.460	2.763	3.23
SLCNT3	25.82	12.91	3.88		3.450	2.101	4.23

In the case of nanocomposites, SL overcomes the limitations of staking fault, crystal structure defect of nanotubes and reduces the inhomogeneity of impurities in pristine MWCNT. However, the concentration of SL impacts the microstructure of nanocomposites. Moreover, the chemically identical shellac molecules and functional groups might be arranged differently on the nanotube surface. As a result, the diffraction pattern is different for SLCNT nanocomposites [41]. It is obvious that the δ increased with increasing SL concentration in the nanocomposite system. Consequently, the crystal size decreased, and the lattice strain increased with increasing SL concentration in the nanocomposites [42]. Therefore, at the lowest concentration (5 wt%) of SL, crystal size extended, the stacking fault and lattice strain reduced. As a result, lattice strain became uniform and improved the crystal flaws in SLCNT1 nanocomposites.

3.6. Thermogravimetric analysis

Fig. 6 depicts the distinguishable thermograms of neat shellac, pristine MWCNT, and SLCNT1, SLCNT2, SLCNT3 nanocomposites. The weight loss at half time of heating and the residue content of those specimens are tabulated in Table S3. The shellac thermogram reveals that shellac decomposed too early as compared to the pristine MWCNT and SLCNT nanocomposites.

It is obvious that there will be a residue nil thermogram at the end of the heating temperature. Therefore, the thermogram of shellac bio-resin affirms that it is a completely combustible material. MWCNT steadily lost weight in the beginning of heating to 386 °C which was sharply falling after 386–695 °C. At the end of the heating, it was partially decayed and finally contained 24.5% residue. The pristine MWCNT contains different amorphous ring carbon, graphite and fullerenes as impurities. Different carbon-carbon bond lengths, edges and dangling bonds exist in those carbon materials that affect the nanotube surfaces and produce defects in the nanotubes. Usually, amorphous carbons and defected nanotubes are decomposed gradually during heating.

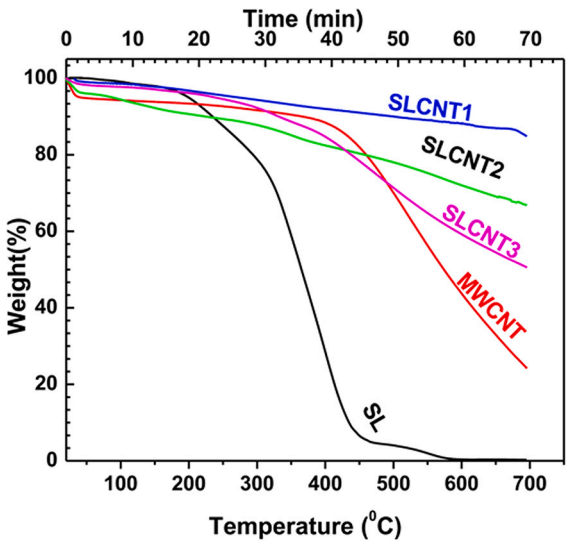

Fig. 6. TGA thermograms of neat shellac, pristine MWCNT, SLCNT1, SLCNT2, SLCNT3.

Additionally, the impurities fused together and evolved at elevated temperatures from the surface of nanotubes which comply with the literature [43,44]. As a result, the weight of pristine MWCNT decays at higher temperature and reduces the thermal stability. Besides, the TGA thermogram of the SLCNT nanocomposites noticeably influenced by the concentration of shellac in the nanocomposite systems. In the case of SLCNT1 nanocomposites which were fabricated with the lowest concentration of shellac, we observed the lowest weight loss approximately in the middle of the heating time and temperature. Moreover, SLCNT1 exhibited the highest half-life with respect to weight loss and residue content. Least amount of shellac was necessary for noticeable dispersion, disentanglement and thermal stability of MWCNT. It suggests that there were improved interaction and network structure between nanotube and shellac in SLCNT1 nanocomposites [35,45]. Also, the yarn like the structure of nanotubes and shellac might act as heat resistant material as stated elsewhere [46]. Conspicuously, during the shellac treatment, the amorphous carbon was removed which probably facilitated higher thermal stability of SLCNT1 compared to pristine MWCNT [47]. Furthermore, a part of shellac perhaps interacted with nanotubes and coated on the nanotube surface, the rest of the shellac conceivably interacted with amorphous carbon materials and other impurities. However, a greater concentration of shellac influenced the interaction mechanism between shellac and amorphous carbon materials to form complex materials. It seems that at higher concentration of shellac, more complex impurities were formed. Consequently, SLCNT2 and SLCNT3 nanocomposites gradually decayed at an extended time and elevated temperature followed by a decrease in the residue content with the increase in the shellac concentration. Finally, they became thermally less stable compared to SLCNT1. Therefore, considering the thermograms of shellac, MWCNT, and SLCNT nanocomposites, 5 wt% shellac is suitable to remove surface flaws, for homogeneous dispersion and long-time stabilization of nanotube suspension for future application.

3.7. ROS formation study

Stress is one of the most important mechanisms of toxicity caused by the administration of nanoparticles which due to their small size and large surface area, can produce ROS and oxidative stress [48]. CNT can cause oxidative stress and result in cellular toxicity due to the formation of free radicals, depletion of antioxidants, and accumulation of peroxidative products which ultimately reduce the viability of cells [49].

Hence, we observed ROS generation due to the treatment of cells by our MWCNTs and SLCNTs. ROS generation is dose-dependent. ROS species (e.g., H_2O_2, superoxide radical, hydroxyl radical) cause damage to cellular components including DNA damage which facilitates apoptotic cell death. Our result shows that functionalization of MWCNTs by shellac could reduce the generation of ROS to a significant extent compared to pristine MWCNTs (Fig. 7(a)).

Impurities can significantly affect radical formation caused by CNTs. A study reported that the presence of iron in CNT in very low amount (0.23 wt% of iron) or high amount (26 wt% of iron) can generate hydroxyl radical in zymosan-stimulated RAW 264.7 cells [50]. MWCNT with high carbon purity (99.79 wt%) also exhibited ROS production and could change cell size [51].

It is evident from the literature that variation in ROS production shown by MWCNT depends on the type and amount of impurities. Our MWCNT has different metals (Co, Fe, Ni, Mo, etc.). During functionalization, some impurities although not all, partially leached. That's why, functionalized SLCNTs showed less ROS production and the result complies with those reported earlier [52,53].

3.8. Cytotoxicity study

To investigate the cytotoxicity of SLCNT and to compare it with that shown by MWCNT, we performed MTT assay (Fig. 7(b)). We varied the concentration of CNTs. Our study shows that except for the smallest concentration investigated which is 5 μg/ml, our functionalized SLCNT is less cytotoxic compared to MWCNT. The maximum dose investigated was 500 μg/ml at which both SLCNT and MWCNT showed significant cytotoxicity. Microscopic observation showed the presence of significant aggregation at 500 μg/ml dose for both MWCNTs and SLCNTs which gives the idea that the high dose is toxic (data not shown here). For small doses (e.g., 5 and 25), our SLCNT showed slight cytotoxicity compared to the control group whereas MWCNT was quite cytotoxic for those doses. The results certainly support that biocompatibility improved due to SL functionalization. Cytotoxicity of CNT is highly dependent on the concentration and specific characteristics of CNTs. The toxicity of CNTs can be affected by the extent of dispersion too. Many studies reported

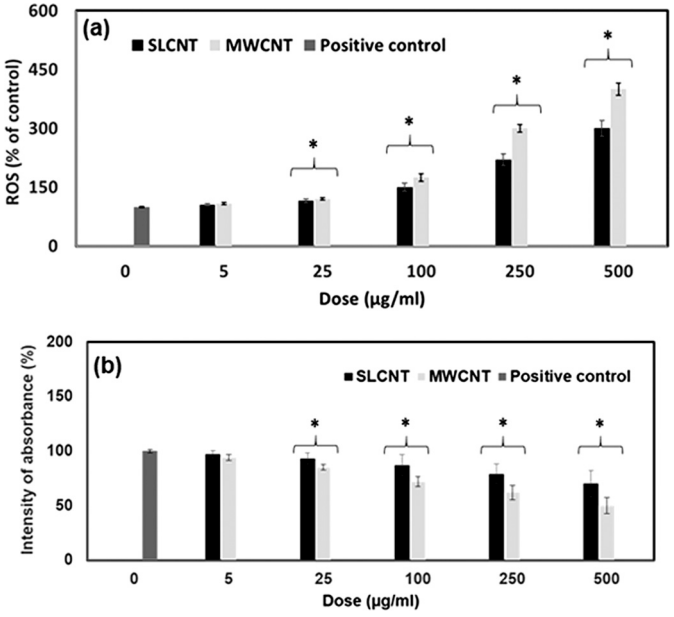

Fig. 7. (a) ROS generation in RAW 264.7 cell following 24 h exposure to various concentrations of SLCNTs and MWCNTs, (b) effect of the SLCNTs and MWCNTs on the viability of RAW 264.7 macrophage cells detected by MTT assay. Data are presented as means ± SD from three independent experiments. The asterisks (*) indicate statistically significant differences compared with MWCNT (*$p < 0.05$).

that appropriate surface coatings can reduce the toxicity of CNTs in vitro and in vivo. Some studies suggest that functionalized CNTs contain less metallic impurities compared to pristine CNTs which can be attributed to less cytotoxicity shown by functionalized CNTs. It was reported that carboxy or amino functionalization can significantly reduce cytotoxicity caused by pristine MWCNTs [53]. Our study also shows a similar trend. MWCNTs can extend the cell membrane of macrophages which ultimately causes membrane rupture [54]. Hence, it was obvious to observe significant cytotoxicity by MWCNT used in our study. Whereas, our functionalization is expected to reduce impurities and improve the solubility of MWCNTs which in turn helped to reduce cytotoxicity.

4. Conclusion

The study reports an attractive way to prepare stable SLCNT dispersion from highly unstable MWCNT using shellac bio-resin. Low cost, natural shellac when used at low concentration (5 wt%), was very effective to stabilize MWCNT for a long time. It was found in our investigation that shellac imparts –COOH and –OH functional groups on the MWCNT surface. The microstructure and the lattice parameters of nanocomposites remarkably improved at a low concentration of SL. The non-covalent functionalization improved the thermal stability of MWCNT, reduced its impurities, and made them less cytotoxic. The improved thermal stability of SLCNT nanocomposites could be a promising characteristic for the heating device. Hence, our nanocomposite is a potent candidate to be used at elevated temperatures and in the biomedical field.

Declaration of Competing Interest

None

Acknowledgements

The authors would like to acknowledge the Ministry of Higher Education, Malaysia for providing financial support through FRGS (RDU 160148) for this project. Dr. Alam is grateful to Bangladesh Atomic Energy Commission, Ministry of Science and Technology, Dhaka, Bangladesh for the official supports.

Appendix A. Supplementary data

Supplementary data to this article can be found online at https://doi.org/10.1016/j.colcom.2021.100395.

References

[1] M.S. Islam, A.N. Naz, M.N. Alam, A.K. Das, J.H. Yeum, Electrospun poly(vinyl alcohol)/silver nanoparticle/carbon nanotube multi-composite nanofiber mat: fabrication, characterization and evaluation of thermal, mechanical and antibacterial properties, Colloid Interface Sci. Commun. 35 (2020) 100247.
[2] S. Kumar, R. Rani, N. Dilbaghi, K. Tankeshwar, K.H. Kim, Carbon nanotubes: a novel material for multifaceted applications in human healthcare, Chem. Soc. Rev. 46 (2017) 158–196.
[3] H. Xu, Y. Sang, B. Xu, L. Zhang, L. Zhang, H. Xu, Immobilization of gold nanoparticles on poly(4-vinylpyridine)-grafted carbon nanotubes as heterogeneous catalysts for hydrogenation of 4-nitrophenol, ACS Appl. Nano Mater. 3 (12) (2020) 12169–12177.
[4] L.-M. Peng, Z. Zhang, S. Wang, Carbon nanotube electronics: recent advances, Mater. Today 17 (2014) 433–442.
[5] R. Poon, I. Zhitomirsky, Application of Cyrene as a solvent and dispersing agent for fabrication of Mn3O4-carbon nanotube supercapacitor electrodes, Colloid Interface Sci. Commun. 34 (2020) 100226.
[6] H.C. Tsai, J.Y. Lin, F. Maryani, C.C. Huang, T. Imae, Drug-loading capacity and nuclear targeting of multiwalled carbon nanotubes grafted with anionic amphiphilic copolymers, Int. J. Nanomedicine 8 (2013) 4427–4440.
[7] N.J. Singhai, R. Maheshwari, S. Ramteke, CD44 receptor targeted 'smart' multi-walled carbon nanotubes for synergistic therapy of triple-negative breast cancer, Colloid Interface Sci. Commun. 35 (2020) 100235.
[8] N.W. Kam, H. Dai, Carbon nanotubes as intracellular protein transporters: generality and biological functionality, J. Am. Chem. Soc. 127 (2005) 6021–6026.
[9] Z. Zhang, X. Yang, Y. Zhang, B. Zeng, S. Wang, T. Zhu, et al., Delivery of telomerase reverse transcriptase small interfering RNA in complex with positively charged single-walled carbon nanotubes suppresses tumor growth, Clin. Cancer Res. 12 (2006) 4933–4939.
[10] N. Rahmati, M. Rahimnejad, M. Pourali, S.K. Muallah, Effective removal of nickel ions from aqueous solution using multi-wall carbon nanotube functionalized by glycerol-based deep eutectic solvent, Colloid Interface Sci. Commun. 40 (2021) 100347.
[11] Y. Lei, Q. Huang, J. Dou, H. Huang, G. Yang, F. Deng, et al., Fast adsorptive removal of cationic organic dye by anionic group functionalized carbon nanotubes with high efficiency, Colloid Interface Sci. Commun. 40 (2021) 100328.
[12] A. Alam, Q.T.H. Shubhra, Surface modified thin film from silk and gelatin for sustained drug release to heal wound, J. Mater. Chem. B 3 (2015) 6473–6479.
[13] Q.T. Shubhra, M. Saha, A. Alam, M. Beg, M.A. Khan, Effect of matrix modification by natural rubber on the performance of silk-reinforced polypropylene composites, J. Reinf. Plast. Compos. 29 (2010) 3338–3344.
[14] E. Mehdipoor, M. Adeli, M. Bavadi, P. Sasanpour, B. Rashidian, A possible anticancer drug delivery system based on carbon nanotube–dendrimer hybrid nanomaterials, J. Mater. Chem. 21 (2011) 15456–15463.
[15] E.M. Di Meo, A. Di Crescenzo, D. Velluto, C.P. O'Neil, D. Demurtas, J.A. Hubbell, et al., Assessing the role of poly(ethylene glycol-bl-propylene sulfide) (PEG-PPS) block copolymers in the preparation of carbon nanotube biocompatible dispersions, Macromolecules 43 (2010) 3429–3437.
[16] Y. Liu, C. Chipot, X. Shao, W. Cai, Solubilizing carbon nanotubes through noncovalent functionalization. Insight from the reversible wrapping of alginic acid around a single-walled carbon nanotube, J. Phys. Chem. B 114 (2010) 5783–5789.
[17] S. Pattanayak, S. Chakraborty, M.M.R. Mollick, I. Roy, S. Basu, D. Rana, et al., In situ fluorescence of lac dye stabilized gold nanoparticles; DNA binding assay and toxicity study, New J. Chem. 40 (2016) 7121–7131.
[18] R.D. Hagenmaier, R.A. Baker, Reduction in gas exchange of citrus fruit by wax coatings, J. Agric. Food Chem. 41 (1993) 283–287.
[19] R.G. McGuire, R.D. Hagenmaier, Shellac coatings for grapefruits that favor biological control of *Penicillium digitatum* by *Candida oleophila*, Biol. Control 7 (1996) 100–106.
[20] M.C. Siebers, X.F. Walboomers, S.C. Leeuwenburgh, J.G. Wolke, J.A. Jansen, Electrostatic spray deposition (ESD) of calcium phosphate coatings, an in vitro study with osteoblast-like cells, Biomaterials 25 (2004) 2019–2027.
[21] K. Ma, Y. Qiu, Y. Fu, Q.-Q. Ni, Improved shellac mediated nanoscale application drug release effect in a gastric-site drug delivery system, RSC Adv. 7 (2017) 53401–53406.
[22] M. Irimia-Vladu, E.D. Głowacki, G. Schwabegger, L. Leonat, H.Z. Akpinar, H. Sitter, et al., Natural resin shellac as a substrate and a dielectric layer for organic field-effect transistors, Green Chem. 15 (2013) 1473–1476.
[23] M. Prawatborisut, F. Seidi, D. Yiamsawas, D. Crespy, PEGylation of shellac-based nanocarriers for enhanced colloidal stability, Colloids Surf. B: Biointerfaces 183 (2019) 110434.
[24] S. Limmatvapirat, C. Limmatvapirat, S. Puttipipatkhachorn, J. Nuntanid, M. Luangtana-Anan, Enhanced enteric properties and stability of shellac films through composite salts formation, Eur. J. Pharm. Biopharm. 67 (2007) 690–698.
[25] X. Wang, D.G. Yu, X.Y. Li, S.W. Bligh, G.R. Williams, Electrospun medicated shellac nanofibers for colon-targeted drug delivery, Int. J. Pharm. 490 (2015) 384–390.
[26] J. Roy, 5 - Formulated drugs 1, in: J. Roy (Ed.), An Introduction to Pharmaceutical Sciences, Woodhead Publishing, 2011, pp. 111–140.
[27] J. Triyono, Y. Rizha, T. Triyono, Characterization of biocomposites of sheep hydroxyapatite (SHA)/shellac/sugar as bone filler material, in: AIP Conference Proceedings Vol. 1945, 2018, 020012.
[28] Q.T.H. Shubhra, A. Oyane, H. Araki, M. Nakamura, H. Tsurushima, Calcium phosphate nanoparticles prepared from infusion fluids for stem cell transfection: process optimization and cytotoxicity analysis, Biomater. Sci. 5 (2017) 972–981.
[29] Q.T.H. Shubhra, A. Oyane, M. Nakamura, S. Puentes, A. Marushima, H. Tsurushima, Rapid one-pot fabrication of magnetic calcium phosphate nanoparticles immobilizing DNA and iron oxide nanocrystals using injection solutions for magnetofection and magnetic targeting, Mater. Today Chem. 6 (2017) 51–61.
[30] A. Kumar, C.K. Dixit, 3 - Methods for characterization of nanoparticles, in: S. Nimesh, R. Chandra, N. Gupta (Eds.), Advances in Nanomedicine for the Delivery of Therapeutic Nucleic Acids, Woodhead Publishing, 2017, pp. 43–58.
[31] A. Fraczek-Szczypta, E. Menaszek, T.B. Syeda, A. Misra, M. Alavijeh, J. Adu, et al., Effect of MWCNT surface and chemical modification on in vitro cellular response, J. Nanopart. Res. 14 (2012) 1181.
[32] M. Abdalla, D. Dean, D. Adibempe, E. Nyairo, P. Robinson, G. Thompson, The effect of interfacial chemistry on molecular mobility and morphology of multiwalled carbon nanotubes epoxy nanocomposite, Polymer 48 (2007) 5662–5670.
[33] S. Soradech, S. Limatvapirat, M. Luangtana-anan, Stability enhancement of shellac by formation of composite film: effect of gelatin and plasticizers, J. Food Eng. 116 (2013) 572–580.
[34] Z. Ying-Chen, W. Hong-Yan, Q. Yi-Ping, Morphology and properties of hybrid composites based on polypropylene/polylactic acid blend and bamboo fiber, Bioresour. Technol. 101 (2010) 7944–7950.
[35] L.Y. Jiang, Macroscopic behavior of carbon nanotube (CNT)-reinforced composite accounting for Interface cohesive force, J. Adhes. 86 (2010) 273–289.
[36] M.D.H. Beg, A.K.M. Moshiul Alam, R.M. Yunus, M.F. Mina, Improvement of interaction between pre-dispersed multi-walled carbon nanotubes and unsaturated polyester resin, J. Nanopart. Res. 17 (2015) 53.

[37] L. Stobinski, B. Lesiak, L. Kövér, J. Tóth, S. Biniak, G. Trykowski, et al., Multiwall carbon nanotubes purification and oxidation by nitric acid studied by the FTIR and electron spectroscopy methods, J. Alloys Compd. 501 (2010) 77–84.
[38] P.W. Chiu, G.S. Duesberg, U. Dettlaff-Weglikowska, S. Roth, Interconnection of carbon nanotubes by chemical functionalization, Appl. Phys. Lett. 80 (2002) 3811–3813.
[39] A.K.M.M. Alam, M.D.H. Beg, R.M. Yunus, M.F. Mina, K.H. Maria, T. Mieno, Evolution of functionalized multi-walled carbon nanotubes by dendritic polymer coating and their anti-scavenging behavior during curing process, Mater. Lett. 167 (2016) 58–60.
[40] A. Nouralishahi, A.A. Khodadadi, Y. Mortazavi, A. Rashidi, M. Choolaei, Enhanced methanol electro-oxidation activity of Pt/MWCNTs electro-catalyst using manganese oxide deposited on MWCNTs, Electrochim. Acta 147 (2014) 192–200.
[41] R.W. Grosse-Kunstleve, P.D. Adams, Substructure search procedures for macromolecular structures, Acta Crystallogr. D Biol. Crystallogr. 59 (2003) 1966–1973.
[42] S.L. Aggarwal, G.P. Tilley, Determination of crystallinity in polyethylene by X-ray diffractometer, J. Polym. Sci. 18 (1955) 17–26.
[43] A. Mahajan, A. Kingon, Á. Kukovecz, Z. Konya, P.M. Vilarinho, Studies on the thermal decomposition of multiwall carbon nanotubes under different atmospheres, Mater. Lett. 90 (2013) 165–168.
[44] D. Bom, R. Andrews, D. Jacques, J. Anthony, B. Chen, M.S. Meier, et al., Thermogravimetric analysis of the oxidation of multiwalled carbon nanotubes: evidence for the role of defect sites in carbon nanotube chemistry, Nano Lett. 2 (2002) 615–619.
[45] S. Ho Park, S. Goo Lee, S.H. Kim, Thermal decomposition behavior of carbon nanotube reinforced thermotropic liquid crystalline polymers, J. Appl. Polym. Sci. 122 (2011) 2060–2070.
[46] B. Schartel, P. Pötschke, U. Knoll, M. Abdel-Goad, Fire behaviour of polyamide 6/multiwall carbon nanotube nanocomposites, Eur. Polym. J. 41 (2005) 1061–1070.
[47] X.X. Zhang, C.F. Deng, R. Xu, D.Z. Wang, Oxidation resistance of multi-walled carbon nanotubes purified with sulfuric and nitric acids, J. Mater. Sci. 42 (2007) 8377–8380.
[48] S. Alarifi, D. Ali, Mechanisms of multi-walled carbon nanotubes-induced oxidative stress and genotoxicity in mouse fibroblast cells, Int. J. Toxicol. 34 (2015) 258–265.
[49] A.A. Shvedova, V. Castranova, E.R. Kisin, D. Schwegler-Berry, A.R. Murray, V. Z. Gandelsman, et al., Exposure to carbon nanotube material: assessment of nanotube cytotoxicity using human keratinocyte cells, J. Toxicol. Environ. Health A 66 (2003) 1909–1926.
[50] V.E. Kagan, Y.Y. Tyurina, V.A. Tyurin, N.V. Konduru, A.I. Potapovich, A.N. Osipov, et al., Direct and indirect effects of single walled carbon nanotubes on RAW 264.7 macrophages: role of iron, Toxicol Lett. 165 (2006) 88–100.
[51] S.F. Ye, Y.H. Wu, Z.Q. Hou, Q.Q. Zhang, ROS and NF-kappaB are involved in upregulation of IL-8 in A549 cells exposed to multi-walled carbon nanotubes, Biochem. Biophys. Res. Commun. 379 (2009) 643–648.
[52] K. Pulskamp, S. Diabaté, H.F. Krug, Carbon nanotubes show no sign of acute toxicity but induce intracellular reactive oxygen species in dependence on contaminants, Toxicol. Lett. 168 (2007) 58–74.
[53] A. Chowdhry, J. Kaur, M. Khatri, V. Puri, R. Tuli, S. Puri, Characterization of functionalized multiwalled carbon nanotubes and comparison of their cellular toxicity between HEK 293 cells and zebra fish in vivo, Heliyon 5 (2019), e02605.
[54] T. Zhang, M. Tang, L. Kong, H. Li, T. Zhang, S. Zhang, et al., Comparison of cytotoxic and inflammatory responses of pristine and functionalized multi-walled carbon nanotubes in RAW 264.7 mouse macrophages, J. Hazard. Mater. 219–220 (2012) 203–212.